Localized heating and thermal characterization of high electrical resistivity silicon-on-insulator sensors using nematic liquid crystals

Oguz H. Elibol,[1] Bobby Reddy, Jr.,[2] and Rashid Bashir[3,a)]
[1]*Birck Nanotechnology Center and School of Electrical and Computer Engineering, Purdue University, West Lafayette, Indiana 47906, USA*
[2]*Micro and Nanotechnology Laboratory and Department of Electrical and Computer Engineering, University of Illinois at Urbana-Champaign, Urbana, Illinois 61801, USA*
[3]*Micro and Nanotechnology Laboratory, Department of Electrical and Computer Engineering, Department of Bioengineering, University of Illinois at Urbana-Champaign, Urbana, Illinois 61801, USA*

(Received 11 June 2008; accepted 8 September 2008; published online 30 September 2008)

We present a method for localized heating of media at the surface of silicon-on-insulator field-effect sensors via application of an ac voltage across the channel and the substrate and compare this technique with standard Joule heating via the application of dc voltage across the source and drain. Using liquid crystals as the medium to enable direct temperature characterization, our results show that under comparable bias conditions, heating of the medium using an alternating field results in a greater increase in temperature with a higher spatial resolution. These features are very attractive as devices are scaled to the nanoscale dimensions. © *2008 American Institute of Physics*.
[DOI: 10.1063/1.2993350]

Localized heating schemes can allow for the spatial and temporal downscaling of temperature dependent reactions for miniaturized lab-on-a-chip. Temperature control at the micro and nanoscale has the potential to enable many applications including control of probe-target interaction,[1,2] selective functionalization of the sensor surfaces,[3] realizing active surfaces,[4] and highly localized polymerase chain reaction (PCR).[5,6] Control of this temperature profile over silicon based field-effect electrical biosensors[7] will add another dimension to the functionality of these devices. For these silicon-based field-effect biosensors, a high resistance is appealing for high sensitivity label-free detection of biomolecules.[8] Electrical Joule heating of high resistance devices is challenging since it requires the application of high electric fields to enable enough current flow to heat the device, which can be highly problematic in fluids. Also, heat transfer to both the substrate and the medium limits the increase in temperature and increases the thermal mass of the system. In this work, we fabricated a silicon-on-insulator field effect sensor[9] as was previously reported[1] [Fig. 1(a) (width of 2 μm and length of 20 μm)] and characterized the surface temperature while heating the surrounding media using two different methods. The device active area is 20 nm in thickness (p type -10^{15} cm^{-2}) with a buried oxide thickness of 400 nm and a p type substrate (10^{15} cm^{-2}). First we investigate the Joule heating of the fluid surrounding the device by passing a direct current [Fig. 1(b)]. Next, we directly heat the surrounding fluid by applying an ac voltage between the device and the substrate [Fig. 1(c)]. Such a direct heating scheme for the localization of the heat profile has been demonstrated using only metal leads and at a larger scale.[10] We used liquid crystal (LC) films as the surrounding medium, which have been used for hot spot detection of integrated circuits,[11] to directly characterize the temperature by observing the film through a polarizer orthogonal to the incident polarized light. Nematic LCs available with various clearing temperatures (transition in optical properties) allow characterization of different surface temperatures. Nematic LC films can allow temperature characterization with high spatial resolution and greater ease compared with other established techniques. For example, infrared thermography cannot be used due to the limits in the resolution and the fluidic environment.[12] Using thermochromic LC beads allows for temperature mapping in fluid[13] but does not provide the spatial resolution needed due to the bead size. Fluorescent dyes in fluid, which have shown to be temperature sensitive and exhibit reversible characteristics,[12,14] could be used; however, due to the highly localized nature of the ac voltage heating, the background fluorescence inhibits accurate characterization of the surface temperature.[15]

In order to characterize the temperature increase achievable by Joule heating of the active area via direct current through the devices [shown in Fig. 1(b)], LCs (Accelerated Analysis, Inc.) were applied by brushing the film onto the devices and still photographs were acquired at different bias conditions [Figs. 2(a)–2(d)]. The power required to reach a specific temperature was quantified by analyzing the average intensity of the devices. The intensity over the active area of the device was correlated with the input power, which revealed the transition voltage. A representative plot is shown in Fig. 2(e). A sigmoidal curve fit was performed, and the inflection point is taken as the voltage that results in a specific temperature above the device. To maximize the conductance through the device, the back gate was biased to 30 V to accumulate the device. The ambient temperature through a heated chuck was modulated to quantify different temperature increases using the same film [Fig. 2(f)]. The average temperature increase in the device was characterized with different transition point LCs and a maximum temperature increase of 14 °C was obtained for a source/drain potential difference of 40 V.

To investigate ac voltage mediated heating, LCs were once again applied to the same devices. Voltages were applied [Fig. 1(c)] using a function generator connected to a rf power amplifier at constant frequency of 100 kHz. Still pho-

a)Electronic mail: rbashir@uiuc.edu.

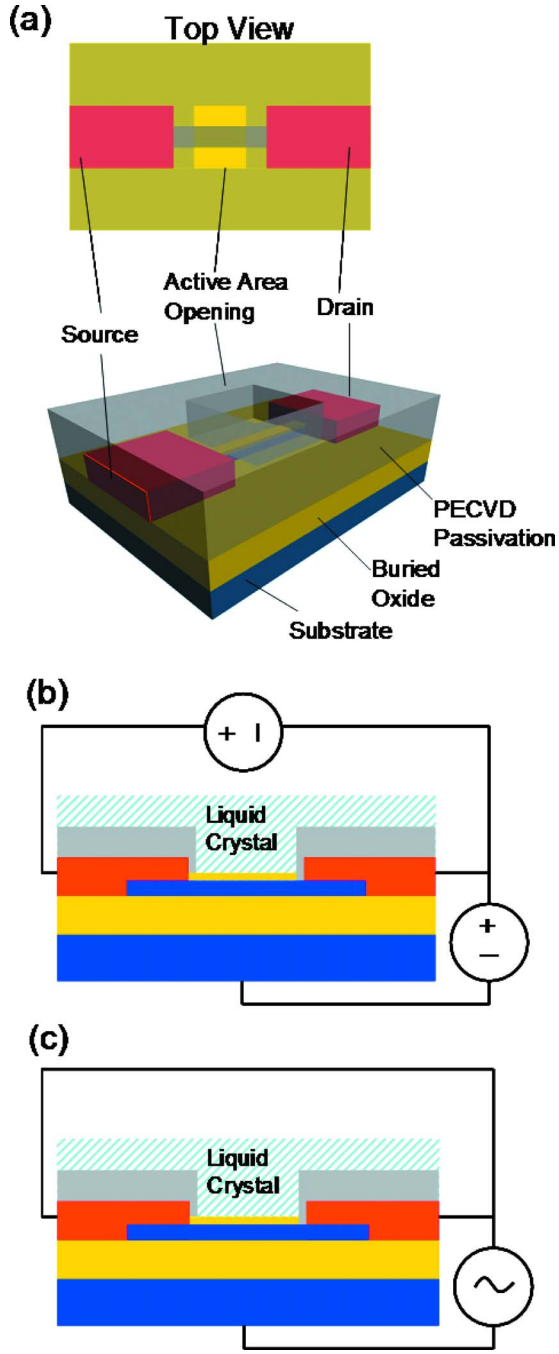

FIG. 1. (Color online) (a) Top and angled schematic of a single device showing the corresponding parts. (b) Schematic of the biasing scheme used for the Joule heating of the device. (c) Schematic of the ac voltage biasing scheme used for the direct heating of the medium.

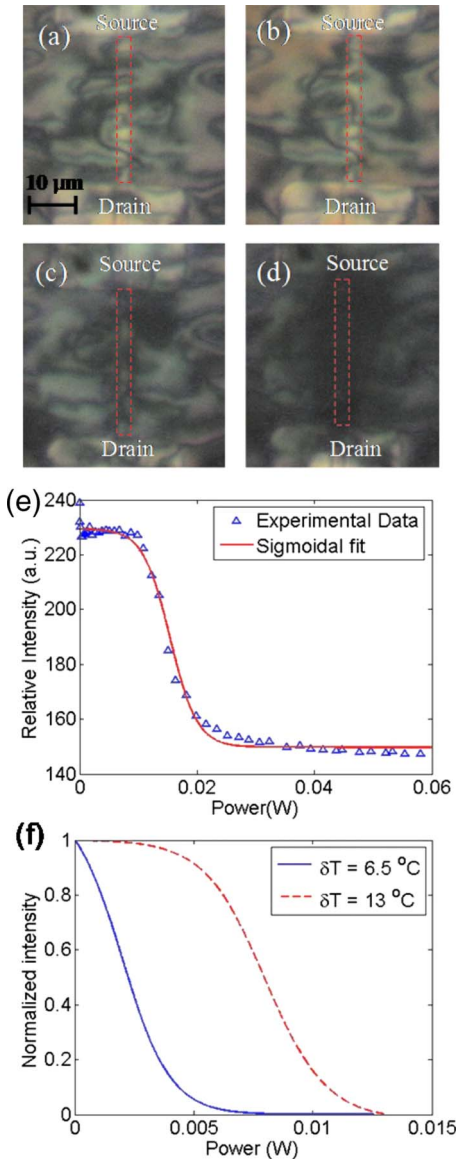

FIG. 2. (Color online) Images showing the device with a coating of 35 °C clearing point LC for Joule heating. The active area has been boxed with red dashed line for clarity. Each micrograph corresponds to different power levels dissipated in the device: (a) 0, (b) 0.85, (c) 3.8, and (d) 5.1 mW. (e) A typical intensity vs input power plot for characterizing the transition temperature. (f) Curves obtained by a sigmoidal fit to the experimental data for two different temperatures obtained utilizing a 35 °C clearing point LC film and modulating the ambient temperature of the device with an external heating chuck.

tographs of a device coated with a specific clearing temperature LC [Figs. 3(a)–3(d)] were acquired and quantified at different bias points [Fig. 3(e)]. LCs with varying clearing temperatures (35, 60.5, and 90 °C) were used to quantify the maximum obtainable temperature. Local heating up to 90 °C at an ambient temperature of 21 °C was observed with the application of 17.5 V_{rms}.

For ac heating, we observe that temperature is confined strictly to the edges of the device with no further propagation. However, the temperature profile originally confined to the 2 μm wide active area diffuses at about 0.8 μm to each side for dc heating from 7 to 14 °C, which is exacerbated by larger increases in temperature. The highly confined temperature profile at the edges of the device for ac heating indicates that the heating is due to the fringing electric field between the active area and the substrate. Dielectric heating dominates over conductive heating due to the high frequencies being used.[16] Using an ac heating technique minimizes the electric field in the medium compared with dc heating techniques, which is crucial for fluidic applications to prevent unwanted reactions or breakdown of insulators. Although the technique still requires finite electric field in the medium, no potential difference exists between the source and drain electrodes for ac heating, whereas a 40 V potential was necessary for dc heating. Furthermore, the peak potential difference needed between the substrate and the source/drain electrode was 25 V for ac heating and about 70 V for dc heating.

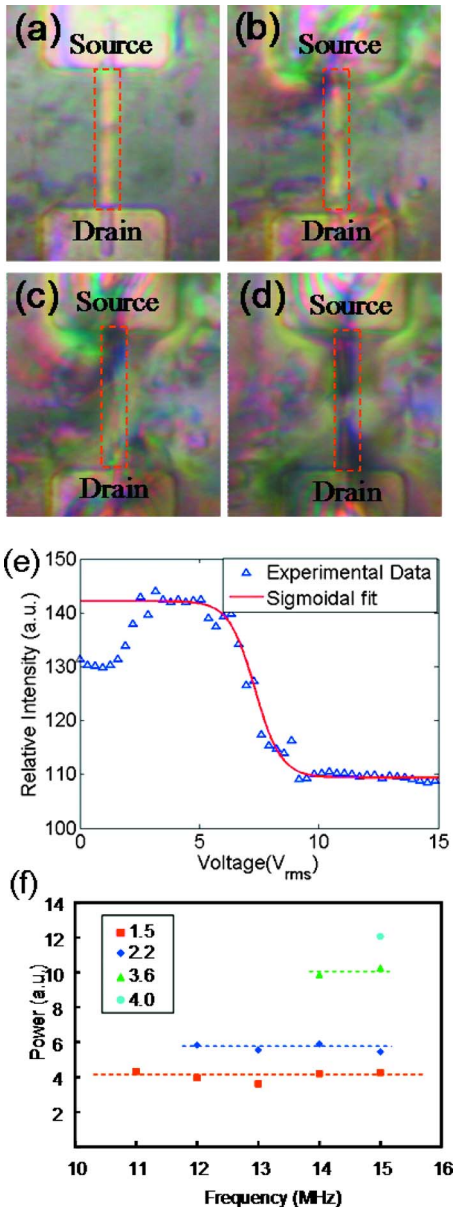

FIG. 3. (Color online) Images showing the device with a coating of 60.5 °C clearing point LC for direct heating of the medium. The active area has been boxed with red dashed line for clarity. Each micrograph corresponds to a different applied bias: (a) 0, (b) 5.6, (c) 11.5, and (d) 17.5 V. (e) A typical intensity vs input power plot for characterizing the transition temperature taken with a 35 °C clearing point LC at an ambient temperature of 21 °C. Initial increase in the average intensity is probably due to the LC responding to the electric field, since a similar increase is seen in the background and was ignored for curve fitting purposes. (f) Product of applied voltage square, frequency, and a complex permittivity assumed to be frequency dependent gives the theoretical power and is plotted against the frequency used for various temperature increases. The dashed lines are included to guide the eyes. The legend contains the temperature increase in degrees Celsius.

To verify that the heating mechanism is indeed due to the direct heating of the medium and to rule out any effect of electric field, the surface temperature of the device was investigated as a function of the applied bias and frequency. A 29 °C clearing temperature LC was applied to the chip, and an external heated chuck was used to control the ambient temperature measured by an external sensor. ac voltages in the range of 10–15 MHz and amplitudes in the range of 0–7 V were used. For dielectric heating, the power dissipated per unit volume is

$$\text{thermal power/volume} = (1/2)|E|^2 \omega \varepsilon_o \varepsilon_r''(\omega), \quad (1)$$

where ω is the frequency in radians, $\varepsilon_r''(\omega)$ is the frequency dependent relative complex permittivity of the dielectric medium, ε_0 is the permittivity of free space, and E is the electric field. The magnitude of the loss parameter depends on the mechanism of the energy loss, which is highly frequency dependent.

For a constant temperature increase, when input power is plotted versus frequency, a curve independent of frequency is expected since input power is correlated with temperature. Plotting $(1/2)|E|^2 \omega \varepsilon_o \varepsilon_r''(\omega)$ versus the frequency for different temperature differences achieved by heating should result in frequency independent curves for different increases in temperature. Figure 3(f) shows the experimental results obtained, assuming a loss tangent that is proportional to $\omega^{2.8}$ for the calculation of theoretical power resulting in a nearly frequency independent behavior. The results indicate that a surface temperature increase is responsible for changes in optical properties of the LCs, instead of side effects of the applied ac voltage.

In conclusion, we use nematic LC films to characterize the surface temperature and quantitatively compare two different heating schemes. We find that it is better to use an ac electric field for the direct heating of the fluid for high resistivity devices as compared with dc voltage for achieving both a larger temperature increase and a higher spatial resolution, which are key considerations as devices continue to be aggressively scaled down. This also allows us to keep the electric field at a minimum to prevent dielectric breakdown and unwanted chemical reactions for applications in fluid. The technique can potentially be used for the direct heating of a wide range of fluids, and the optimum operating frequency will depend on the characteristic of the fluid. Further experimental and simulation work is underway for characterizing the heating of fluids using the ac technique. Direct heating of fluids in a localized fashion, as demonstrated in this work, has many technological applications in lab-on-a-chip systems, such as achieving densely integrated active surfaces or localized PCR modules with built-in sensors.

[1] O. H. Elibol, B. Reddy, Jr., P. R. Nair, M. A. Alam, D. E. Bergstrom, and R. Bashir, NSTI-Nanotech, 2007, Vol. 2, p. 198.
[2] J. SantaLucia, Jr., Proc. Natl. Acad. Sci. U.S.A. **95**, 1460 (1998).
[3] I. Park, Z. Li, A. P. Pisano, and R. S. Williams, Nano Lett. **7**, 3106 (2007).
[4] D. L. Huber, R. P. Manginell, M. A. Samara, B. Kim, and B. C. Bunker, Science **310**, 301 (2003).
[5] M. U. Kopp, A. J. De Mello, and A. Manz, Science **280**, 1046 (1998).
[6] C. Zhang and D. Xing, Nucleic Acids Res. **35**, 4223 (2007).
[7] Y. Cui, Q. Wei, H. Park, and C. M. Lieber, Science **293**, 1289 (2001).
[8] P. R. Nair and M. A. Alam, Nano Lett. **8**, 1281 (2008).
[9] O. H. Elibol, B. Reddy, Jr., and R. Bashir, Appl. Phys. Lett. **92**, 193904 (2008).
[10] J. J. Shah, S. G. Sundaresan, J. Geist, D. R. Reyes, J. C. Booth, M. V. Rao, and M. Gaitan, J. Micromech. Microeng. **17**, 2224 (2007).
[11] H. C. Lin, M. Khan, and T. Giao, Proceedings of the 20th Symposium for Testing and Failure Analysis, 1994, Vol. 81.
[12] H. F. Arata, P. Low, K. Ishizuka, C. Bergaud, B. Kim, H. Noji, and H. Fujita, Sens. Actuators B **117**, 339 (2006).
[13] A. Iles, R. Fortt, and A. J. de Mello, Lab Chip **5**, 540 (2005).
[14] D. Ross, M. Gaitan, and L. E. Locascio, Anal. Chem. **73**, 4117 (2001).
[15] O. H. Elibol, B. Reddy, Jr., P. R. Nair, F. Butler, R. V. Rozhkov, D. Zemlyanov, D. E. Bergstrom, M. A. Alam, and R. Bashir (unpublished).
[16] Y. Yin, S. V. Shiyanovskii, and O. D. Lavrentovich, J. Appl. Phys. **100**, 024906 (2006).